PHYSICAL REVIEW A, VOLUME 61, 032718

Neutral fragmentation of superexcited oxygen molecules

A. Karawajczyk, P. Erman, E. Rachlew-Källne, J. Rius i Riu, M. Stankiewicz,* and K. Yoshiki Franzén
Physics Department I, Royal Institute of Technology, S-10044 Stockholm, Sweden

L. Veseth
Department of Physics, University of Oslo, N-0316 Oslo, Norway

(Received 6 July 1999; published 16 February 2000)

The mechanisms of neutral dissociation of oxygen molecules in the excitation energy range 15–25 eV have been studied in a dispersed fluorescence experiment. By detecting the fluorescence from excited oxygen atoms, we find that neutral superexcited O_2 states below 20 eV dissociate into $O(g.s.)+O(3s,3p)$. At higher excitation energies ($h\nu=20–25$ eV) the curve-crossing interactions following excitations to members of the Rydberg $c\,^4\Sigma_u^-$ series also yield atoms in Rydberg states $(nl, n\geqslant 4)$. The experimental data are analyzed on the ground of many-body perturbation theory, calculations which indicate the structure of the predissociating states converging to the experimentally observed ones.

PACS number(s): 33.50.Dq, 33.80.Gj, 33.80.Rv

I. INTRODUCTION

The processes of neutral fragmentation of the O_2 molecule have attracted much attention in the literature, and the effort has been closely related to atmospheric and astrophysical research (see, e.g., [1–3] and references therein). So far a rather comprehensive understanding of the mechanisms of neutral dissociation in this molecule has been obtained for excitations below the ionization potential (Ref. [4] and references therein). In that energy range the structure of the interacting states has been completely identified. At higher excitation energies the formation of neutral oxygen atoms following high-energy photon excitation has originally been observed in undispersed UV fluorescence [5,6] and photoelectron [7,8] measurements. More recently, dispersed UV fluorescence was measured [9,10] and the data have clarified fragmentation mechanisms following excitations to the members of the Rydberg series converging to the $O_2^+(c\,^4\Sigma_g^-)$ state [R(c) series]. Although, the formation of excited O* atoms at excitations to neutral states occurring in the lower-energy region (16–20 eV) was also observed, the structure of the levels involved in these reactions was not fully explained [9,10]. Actually, the mutual curve-crossing interactions occurring between the bound and repulsive Rydberg levels were suggested to be a primary mechanism leading to molecular fragmentation.

In this paper we report on dispersed fluorescence measurements in the visible and near visible spectral regions (400–950 nm) to identify emission from atomic fragments. By observing emission from transitions between excited states we obtain complementary information to that obtained in the UV fluorescence measurements [9,10]. In these measurements a small bandwidth of the exciting radiation is particularly important so that selective observation from close-lying states can be recorded. Moreover, the measurements also allow us to monitor the formation of atoms in metastable states (with respect to the ground state) such as $2p\,^1S$, $2p\,^1D^o$, and $3s\,^5S^o$, i.e., observations of processes yielding atoms in quintet states have been possible. In fact, dissociation to the $O(3p\,^5P)+O(g.s.)$ limit appears to be the most intense process observed in the present experiment.

To help analyze the experimental data we have carried out *ab initio* computations with the objective of identifying excited molecular states that might lead to either direct dissociation or predissociate precursor (Rydberg) states. Our basic assumption here is that molecular Rydberg states or states of mixed valence-Rydberg character will dissociate to higher atomic limits rather than the rather low ones of present interest. Thus, among the rather large multitude of molecular states we have to try to identify those that are of valence character, tending to the actual dissociation limits in a diabatic manner. In the current energy region above the ionization limit (15–20.5 eV) there so far seems to be neither other *ab initio* studies nor unambiguous experimental observations of the valence type of states.

II. EXPERIMENT

The experiment was performed at the beamline 52 at the Swedish national synchrotron facility MAX-I in Lund utilizing the experimental setup, which has been described in our recent papers [11,12]. Briefly, the synchrotron radiation was dispersed by a 1 m normal incidence monochromator, whose resolution was adjusted to 2 Å (65 meV at $h\nu=20$ eV). The light was transmitted to the experimental chamber, where an ambient pressure of 3×10^{-2} mbar of the O_2 gas was maintained. The emitted fluorescence was gathered by a light collecting system and analyzed by a 0.5 m Jobin-Yvon spectrometer equipped with a 600 line/mm grating and a liquid nitrogen cooled charge coupled device (CCD) detector. The resolution of this spectrometer was adjusted to 0.2–1 nm. The dispersed fluorescence spectra in the wavelength region 400–950 nm have been studied for the energy of the synchrotron photons of 15–25 eV (500–825 Å). The separation between the excitation energies was typically 4 Å (70–200 meV). Intensities of the emission lines were corrected for the

---

*Permanent address: Instytut Fizyki Mariana Smoluchowskiego, Jagiellonian University, Reymonta 4, Kraków, Poland.

1050-2947/2000/61(3)/032718(7)/$15.00

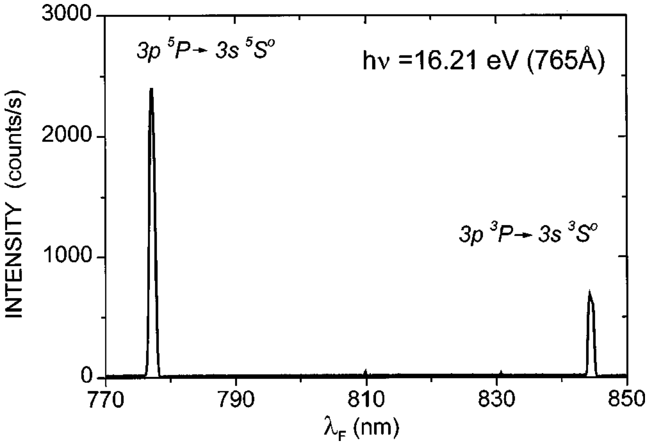

FIG. 1. Dispersed fluorescence spectrum from O_2 recorded at the photon excitation energy 16.21 eV (765 Å). The spectrum shows pronounced O I $3p\ ^3P \rightarrow 3s\ ^3S$ and $3p\ ^5P \rightarrow 3s\ ^5S$ emission lines.

changes of the synchrotron light intensity and variations of the gas pressure by using normalization provided by simultaneously monitoring the strong emission lines of the $O_2^+(b\ ^4\Sigma_g^- — a\ ^4\Pi_u)$ molecular system. In Fig. 1 we present a typical dispersed fluorescence spectrum showing the pronounced $O(3p\ ^5P \rightarrow 3s\ ^5S)$ and $O(3p\ ^3P \rightarrow 3s\ ^3S)$ lines. Other apparatus effects, like the CCD detector quantum efficiency, have been taken into account. Finally, from the experimental data we have derived the formation ratio ξ_{nl} defined as the number of molecules dissociating into $O(nl)$ $+O$. For each excitation energy the value of ξ_{nl} is obtained from the intensity of the respective fluorescence line using the formula $\xi_{nl} = (I_{nl}/\tau)A_{ik}$, where I_{nl} denotes the number of recorded photons, τ is the lifetime of the nl state, and A_{ik} the transition probability of the transition in question. Provided that the level in question is not additionally populated via cascade transitions from higher excited states, the function ξ_{nl} is a measure of the relative cross section for dissociation into a considered channel. The role of the cascade transitions will be explicitly discussed for the cases where such processes have been experimentally observed.

The Grotrian diagram of the observed emission lines is shown in Fig. 2 in which we also include the UV transitions reported in Refs. [9,10].

III. THEORY

To help identify the mechanism behind the observed fragmentation processes, we have computed excitation energies within the ground-state Franck-Condon region for a series of singly and doubly excited states of the neutral molecule. The present method of calculation is a many-body approach for general model spaces, which has been described in detail elsewhere [12,13]. At the heart of the method is an effective Hamiltonian in the form of a perturbation series, which in the present application is complete to second order. The energies are obtained by diagonalizing the effective Hamiltonian matrix within a model space consisting of a number of chosen configurations, and interactions with all other configurations

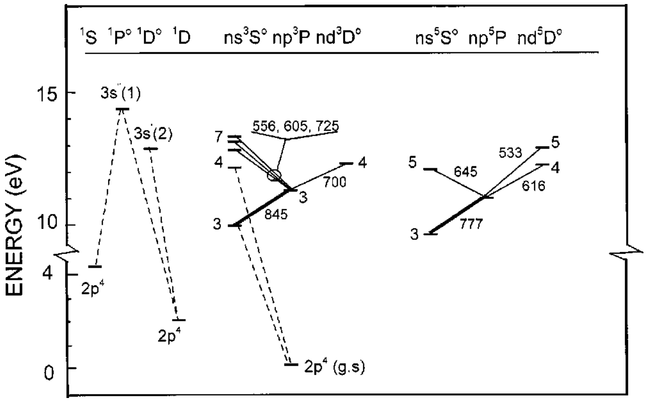

FIG. 2. Diagram of the experimentally observed atomic emission lines. Dashed lines: the UV emission recorded in Refs. [9,10]. Thick lines: the near visible emission observed in the entire studied excitation energy region in the present experiment. Thin lines: visible emission lines exclusively found at excitations of the neutral states in the region of the R(c) Rydberg series.

are included in the matrix to second order in the electronic repulsion operator. Thus, a comprehensive inclusion of dynamic correlation effects should be ensured.

Molecular orbitals were constructed using Slater atomic orbitals of s-, p- and d-symmetries ($n=1,2,3$), with several diffuse orbitals added for each symmetry to enable a (limited) inclusion of molecular orbitals of Rydberg character. The calculations were based on a total of 24 molecular orbitals of σ-symmetry, 16 of π-symmetry, and 10 of δ-symmetry. The two lowest excited (virtual) orbitals of σ_g-symmetry ($4\sigma_g$ and $5\sigma_g$) were found to be localized, i.e., of valence type, and the same applies to the first excited ones of π_u- and π_g-symmetry, i.e., the $2\pi_u$ and $2\pi_g$ orbitals. However, the two lowest excited orbitals of σ_u-symmetry ($3\sigma_u$ and $4\sigma_u$) were found to be rather delocalized, i.e., of Rydberg character. It should be recalled here that the molecular orbitals are based on a two-center expansion, so there is no direct correspondence between a molecular Rydberg orbital and any particular Slater orbital from the basis set.

The objective of the present calculations is to identify molecular states of various symmetries that dissociate to the atomic limits $O(3p\ ^3P)+O(g.s.)$ and $O(3p\ ^5P)+O(g.s.)$ with subsequent prominent O I emission as shown in Fig. 1. For that purpose we will assume that molecular states of Rydberg character, i.e., states containing excitations to Rydberg orbitals, dissociate to higher atomic limits. Thus, when computing molecular excitation energies we want to identify those that are of valence type, which are then successively correlated with the lowest atomic dissociation limits according to the Wigner-Witmer rules [14]. This procedure basically enables a diabatic correlation between atomic states and molecular states at vertical excitation from the ground state. Another procedure could be to discard all (extra) diffuse Slater orbitals in the basis set and thereby also molecular orbitals of Rydberg character. In this way we can make an adiabatic correlation involving only the valence states. However, the latter procedure might certainly be less accurate, as the valence-Rydberg interactions are neglected. We will comment on this point in Secs. IV B and IV C.

Molecular states above the ionization limit are generally unstable against autoionization. In the perturbation expansion this is manifested in the form of singularities which requires special attention. This feature combined with the high density of states makes it very difficult and laborious to compute potential curves over wide ranges of internuclear separations. Other, more standard quantum chemistry methods based on variational techniques tend to meet large problems of instabilities in this energy region.

Our many-body approach also enables computations of transition probabilities (dipole strengths) for allowed electric dipole transitions from the ground state. Such information is important when we want to investigate whether direct dissociation is a probable mechanism. Furthermore, lifetimes for autoionization can also be computed, giving useful information on the competing processes dissociation/autoionization for repulsive states above the ionization limit.

IV. PREDISSOCIATIONS IN THE REGION 15–20.5 eV

Our observed dispersed fluorescence spectra acquired below 20 eV excitation energy reveal two strong emission lines at 845 nm $[\mathrm{O}(3p\,^3P)\rightarrow\mathrm{O}(3s\,^3S)]$, and at 777 nm $[\mathrm{O}(3p\,^5P)\rightarrow\mathrm{O}(3s\,^5S^0)]$. In the same energy range population, $\mathrm{O}(3s''\,^1P^o)$, $\mathrm{O}(3s'\,^1D^o)$, and $\mathrm{O}(3s\,^3S^o)$ have been observed in UV fluorescence measurements [9]. Two main mechanisms leading to neutral dissociation have to be considered: direct excitation to a (repulsive) molecular state, or excitation to a (Rydberg) state followed by a spin-allowed predissociation via another (valence) state. Weak spin-forbidden versions of these two processes might also be observed. As discussed in the theory section we want to identify the mediators of the observed neutral dissociations, i.e., the valence states converging to the $\mathrm{O}(3p\,^5P)+\mathrm{O}(\mathrm{g.s.})$ and $\mathrm{O}(3p\,^3P)+\mathrm{O}(\mathrm{g.s.})$ limits.

A. The neutral precursor states

The $3p\,^5P$ and $3p\,^3P$ formation functions are shown in Figs. 3(a) and 3(b), respectively. The $3p\,^5P$ curve has been normalized to unity at $h\nu=16.21$ eV (765 Å) and the remaining nl functions have been rescaled accordingly. We note that all resonances recorded in the $3p\,^5P$ curve are also visible in the $3p\,^3P$ curve. Also, the onsets in Figs. 3(a) and 3(b) coincide with the thermodynamical thresholds for dissociation to the respective limits. This leads to the conclusion that at least one of the predissociating states must be attractive and exhibit a potential minimum at higher internuclear distances.

In the excitation region 17–19 eV (605–729 Å) both curves show a distinct structure originating from predissociations of the Rydberg series converging to the $\mathrm{O}_2^+(b\,^4\Sigma_g^-)$ and the $\mathrm{O}_2^+(B\,^2\Sigma_g^-)$ states [the R(b) and R(B) series, respectively]. The positions of these Rydberg states are tentatively marked in Figs. 3(a) and 3(b). The $n=4$ members of the R(b) progression and $n=4,5,6$ of the R(B) progression are partially resolved. Higher Rydberg levels constitute broad features visible in Figs. 3(a) and 3(b) below the ionization limits of these series.

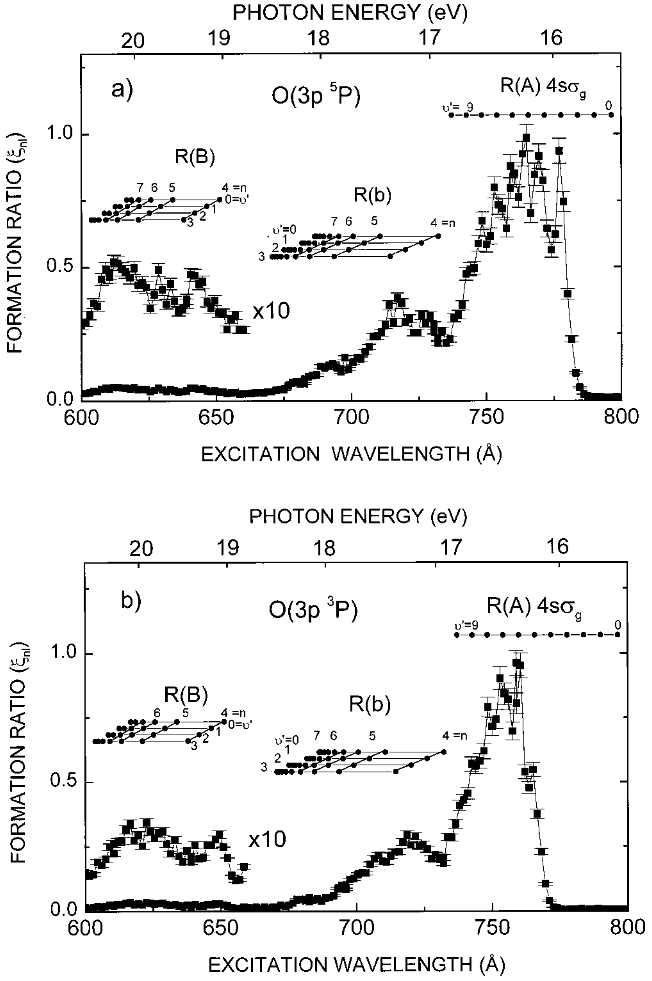

FIG. 3. The ratio ξ_{nl} of formation of atoms in the $3p\,^5P$ (a) and $3p\,^3P$ (b) states in the energy region 15.5–19.1 eV, 650–800 (Å).

The strongest resonances are observed at 15.9–16.9 eV (735–780 Å). Possible precursor states are expected to be members of the Rydberg series converging to the $\mathrm{O}_2^+(A\,^2\Pi_u)$ state [R(A) series]. The structure of the $3s\sigma_g$ member of this series has been analyzed previously [15] using different isotopic $^{16}\mathrm{O}_2$, $^{16}\mathrm{O}^{18}\mathrm{O}$, and $^{18}\mathrm{O}_2$ targets. Using the derived constants [15] for this state we have calculated the expected positions of higher members of the series. As seen from Fig. 3(a) there is a reasonable agreement between the measured resonances and the calculated positions of the vibrational levels of the R(A) $4s\sigma_g$ state.

B. Dissociations into $\mathrm{O}(3p\,^5P)+\mathrm{O}(\mathrm{g.s})$

There are two states of $^3\Pi_u$ symmetry that converge to the $\mathrm{O}(3p\,^5P)+\mathrm{O}(\mathrm{g.s})$ limit. Their computed vertical excitation energies are 15.4 eV (805 Å) and 15.6 eV (795 Å), respectively, (cf. Table I). Both states tend to be attractive with equilibrium distances outside the Franck-Condon region (cf. Table I). The transition probability (dipole strength) for excitation to the state at 15.6 eV is fairly large ($|\vec{r}_{ai}|^2=0.044$ a.u.), and this state which has a leading configura-

TABLE I. Computed properties of molecular triplet valence states of *u*-symmetry that converge to the atomic limits $\mathrm{O}(3p\ ^5P)+\mathrm{O(g.s.)}$, and $\mathrm{O}(3p\ ^3P)+\mathrm{O(g.s.)}$ respectively. Computations are carried out at $R=2.282$ a.u. ΔE indicates the spread in excitation energies over the ground-state Frank-Condon (FC) region ($R=2.19$ a.u.–$R=2.37$ a.u.). $|\vec{r}_{ai}|^2$ denotes the dipole strength [13] for allowed electric dipole transitions from the ground state. * Indicates vertical excitation energies computed with neglect of valence-state–Rydberg-state interactions (reduced basis, cf. Sec. III).

		Vertical excitation energy (eV)	Vertical excitation energy (eV)*	ΔE (FC region)	$\|\vec{r}_{ai}\|^2$ (a.u.)	Dominant excitation
$\mathrm{O}(3p\ ^5P)$	$^3\Delta_u$	20.4	20.3	21.2 – 19.7		$2\sigma_u\rightarrow 4\sigma_g+3\sigma_g 1\pi_u\rightarrow 1\pi_g 4\sigma_g$
	$^3\Sigma_u^+$	20.7	21.5	22.0 – 20.0		$3\sigma_g 1\pi_u\rightarrow 1\pi_g, 4\sigma_g$
	$^3\Sigma_u^+$	20.6	20.5	21.5 – 19.8		$2\sigma_u\rightarrow 4\sigma_g+3\sigma_g 1\pi_u\rightarrow 1\pi_g 4\sigma_g$
	$^3\Sigma_u^-$	18.9	19.1	19.4 – 18.4	0.037	$2\sigma_u\rightarrow 4\sigma_g$
	$^3\Pi_u$	15.6	15.8	17.1 – 14.9	0.044	$3\sigma_g 1\pi_u\rightarrow 1\pi_g^2$
	$^3\Pi_u$	15.4	15.6	16.8 – 14.6	0.0075	$1\pi_u\rightarrow 4\sigma_g$
$\mathrm{O}(3p\ ^3P)$	$^3\Delta_u$	20.6	21.1	21.7 – 19.8		$3\sigma_g 1\pi_u\rightarrow 1\pi_g 4\sigma_g$
	$^3\Sigma_u^+$	22.8	23.4	23.8 – 21.8		$1\pi_u^2\rightarrow 1\pi_g 2\pi_u+3\sigma_g^2\rightarrow 1\pi_g 2\pi_u$
	$^3\Sigma_u^+$	21.5	22.3	23.0 – 20.2		$1\pi_u^2\rightarrow 1\pi_g 2\pi_u$
	$^3\Sigma_u^-$	20.3	20.5	21.4 – 19.7	0.00003	$3\sigma_g 1\pi_u\rightarrow 1\pi_g 4\sigma_g+2\sigma_u\rightarrow 4\sigma_g$
	$^3\Pi_u$	17.4	17.6	18.4 – 16.5	0.0015	$1\pi_u\rightarrow 4\sigma_g+1\pi_u\rightarrow 5\sigma_g$
	$^3\Pi_u$	17.3	17.3	18.3 – 16.5	0.036	$1\pi_u\rightarrow 4\sigma_g+1\pi_u\rightarrow 5\sigma_g$

tion $3\sigma_g 1\pi_u^3 1\pi_g^4$ is fairly stable against autoionization, our computed autoionization lifetime is 1.5×10^{-13} s. Therefore, excitation of this state in the energy region from the $\mathrm{O}(3p\ ^5P)+\mathrm{O(g.s.)}$ limit and up to about 17 eV (Franck-Condon region, cf. Table I) might be expected to lead to neutral dissociation of the O_2 molecule. However, we have to emphasize that direct excitation and subsequent dissociation of this valence state cannot be the origin of the narrow resonances observed at 16–17 eV [cf. Fig. 3(a)]. Excitation to the $^3\Pi_u$ state at 15.4 eV tends to be negligible due to a small transition probability ($|\vec{r}_{ai}|^2=0.0075$ a.u., see Table I). Direct dissociation via the $^3\Sigma_u^-$ state at the vertical energy 18.9 eV (leading configuration $2\sigma_u\rightarrow 4\sigma_g$) also seems to be weak in spite of a significant transition probability ($|\vec{r}_{ai}|^2=0.037$ a.u., see Table I). Our calculations indicate, however, that this state will most likely decay via autoionization, as its computed autoionization lifetime is as short as 2.5×10^{-14} s.

The $^3\Delta_u$ state and the two $^3\Sigma_u^+$ states that converge to the $\mathrm{O}(3p\ ^5P)+\mathrm{O(g.s.)}$ limit (cf. Table I) may predissociate precursor (Rydberg) states through spin-allowed processes. All these three states have strong admixtures of doubly excited valence type configurations, and their computed vertical excitation energies are as high as 20.4 eV, 20.6 eV, and 20.7 eV, respectively. Thus, these states are expected to predissociate the R(A), R(b), and R(B) Rydberg states, and the interaction will take place outside the Franck-Condon region.

From Table I we see that the two methods discussed in Sec. III to compute vertical excitation energies for the valence states yield quite consistent results. The present discussion is, however, based on the results obtained from the most comprehensive computation that includes the valence-Rydberg-state interaction (large basis with diffuse atomic orbitals included).

C. Dissociations into $\mathrm{O}(3p\ ^3P)+\mathrm{O(g.s.)}$

As for the $\mathrm{O}(3p\ ^5P)+\mathrm{O(g.s.)}$ limit there are six molecular states of triplet- and *u*-symmetry that converge to the $\mathrm{O}(3p\ ^3P)+\mathrm{O(g.s.)}$ limit. The two states of $^3\Pi_u$ symmetry and the one of $^3\Sigma_u^-$ symmetry (computed vertical excitation energies 17.3 eV, 17.4 eV, and 20.3 eV, respectively, cf. Table I) can be reached by electric dipole transitions from the ground state, and may lead to a direct dissociation. However, for the upper $^3\Pi_u$ (17.4 eV) and the $^3\Sigma_u^-$ state the computed transition probabilities ($|\vec{r}_{ai}|^2=0.0015$ a.u. and 0.000 03 a.u., respectively) are too small to favor direct dissociations. For the lower $^3\Pi_u$ state (at 17.3 eV) the computed transition probability is of a more reasonable magnitude ($|\vec{r}_{ai}|^2=0.036$ a.u.), and direct dissociations might be expected within the Franck-Condon region of energies (16.5 eV–18.3 eV, cf. Table I). According to our computed values the lower as well as the upper $^3\Pi_u$ states tend to be bound states (dissociation limit ~ 16.0 eV). However, both of them undergo rather fast autoionization to the ionic ground state, and our computed autoionization lifetimes are for both of them approximately 7×10^{-14} s. Thus, autoionization is expected to be the dominant decay mechanism.

Hence, in conclusion it might be stated that our computed results do not point to direct dissociation to the $\mathrm{O}(3p\ ^3P)+\mathrm{O(g.s.)}$ limit as an important mechanism. Spin-allowed predissociations of the precursor Rydberg state R(A), R(b), and R(B) by the triplet states listed in Table I seem to be the most plausible explanation for the observed fragmentation in this case. The many narrow structures observed in the strong resonance in the region 16.0–16.5 eV is also a clear sign of precursor Rydberg states [cf. Fig. 3(b)].

As in the case of the O($3p\,^5P$)+O(g.s.) limit we notice from Table I that the vertical excitation energies computed with the large basis set with allowance for valence-state–Rydberg-state interactions, are quite consistent with the results obtained with a reduced valence type of basis set. We consider this consistency as a verification of our assumption that molecular states of valence type can be identified and correlated with the present two dissociation limits in an unambiguous diabatic manner. Unfortunately, there seem to be neither other unambiguous observations of valence type vertical excitation energies in the energy region above 15 eV nor other calculations for comparison. We have, however, also computed vertical excitation energies for the lowest few excited $^3\Sigma_u^-$ and $^3\Pi_u$ states in the region 8.5–12 eV. Even in this low-energy region there are rather few opportunities to make comparisons with other computed vertical energies but our results compare very well (within 0.3 eV) with, e.g., the results of Buenker and Peyerimhoff [16].

We have not considered the possibility of (weak) spin-forbidden dissociation mechanisms. Our calculations yield quintet states with vertical excitation energies in the relevant regions that also converge to the O($3p\,^5P$) and O($3p\,^3P$) dissociation limits. Singlet states converging to the actual limits have all according to our computed results too low excitation energies to be of interest. Our observed results in the energy region 15–20.5 eV, however, do not seem to justify any further discussion of spin-forbidden processes.

V. THE REGION OF THE R($c\,^4\Sigma_u$) SERIES (20.5–25 eV)

From Table I we see that spin-allowed direct dissociations to the limits O($3p\,^5P$)+O(g.s.) or O($3p\,^3P$)+O(g.s.) are not expected to occur for energies above 21 eV. Furthermore, our computed results do not even favor spin-allowed predissociation to the O($3p\,^5P$)+O(g.s.) limit in this high-energy region. Thus, different mechanisms have to be considered to explain the clearly observed resonance in the O($3p\,^5P$) spectrum at 22.3 eV [cf. Fig. 4(a)] which is almost absent in the O($3p\,^3P$) spectrum [Fig. 4(b)]. One explanation that should be taken into account is that the second atom might be in an excited state after the dissociation, e.g., O($2p\,^1D$) or O($2p\,^1S$). Due to the high density of states we find it quite infeasible to extend our correlation diagrams to such high dissociation limits.

The dynamics of the neutral fragmentation following excitation of the members of the R(c) series differs from what was observed at the lower-lying Rydberg series. Besides the emission from the $3p\,^{3,5}P$ states we have detected fluorescence from the O(nl) Rydberg states ($n \geqslant 4$) (Fig. 5), which indicates an involvement of repulsive molecular Rydberg states. The R(c) potential curve is very shallow with a barrier hosting only two vibrational levels $v'=0,1$. Predissociation from the $v'=0$ level is slow because of the width of the barrier, while as recently shown [10], the $ns\sigma_g$, $v'=1$ member of the R(c) series dissociate to the O($ns\,^3S$)+O($2p\,^1D$) limit by tunneling through the potential barrier. The fragmentation occurs via the potential curve of this Rydberg state, which leads to the preservation of the principal quantum number of the Rydberg electron during fragmentation. The occurrence of a similar propensity rule in the dissociation of the nd Rydberg series has been suggested in Ref. [10].

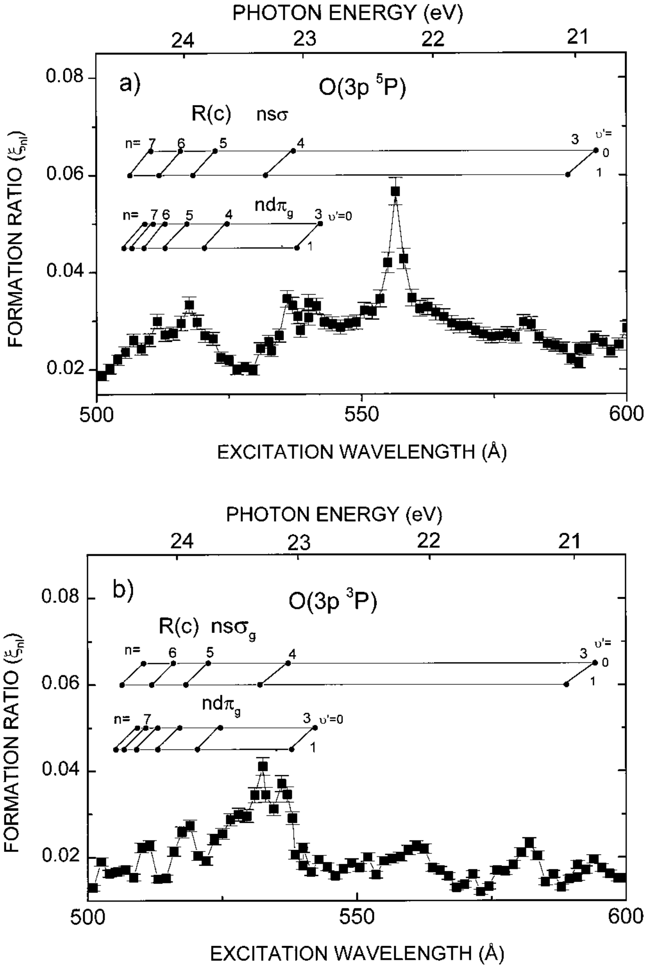

FIG. 4. The ratio ξ_{nl} of the formation of atoms in the $3p\,^5P$ (a) and $3p\,^3P$ (b) states in the energy region 19.1–24.8 eV, 650–800 Å.

For comparison with Refs. [9,10] we have also recorded O($ns\,^3S^0$; $n=5-7$)→O($3p\,^3P$) emission lines at excitation to the respective molecular R(c) $ns\sigma_g$, $v'=1$ states ($n=5-7$). The emission from the O($4s\,^3S^0$) state occurs at 1316.4 nm, which is outside the sensitivity range of our detector and has therefore not been observed. These results are examplified by the $6s$ function shown in Fig. 5(a). Clearly, the propensity rule proposed in Ref. [10] holds in this case; the fluorescence from the O($6s\,^3S^0$) state is strong at top of the R(c) $6s$ $v'=1$ resonance and very weak at higher members of the ns progression. However, the conservation of the principal quantum number does not occur in decay of the ns and nd states to the O($nd\,^3D^0$)+O(g.s.) limits for the following reasons. First, we have observed emission from the O($ns\,^3D$), $n=4,5,6$ levels [see Fig. 5(b)], which has not been observed in the UV spectra probably due to limited resolution. The spectrum of Fig. 5(b) shows that emission

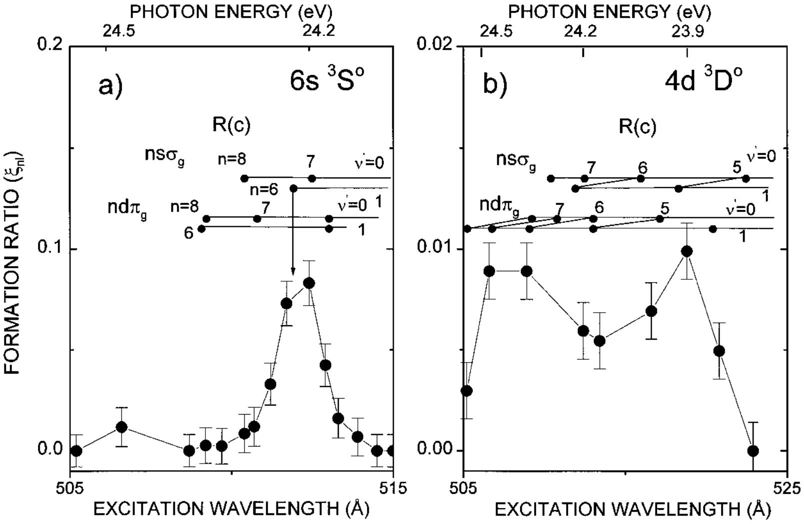

FIG. 5. The ratio ξ of formation of atoms in the $6s\ ^3S$ (a) and $4d\ ^3D^{\ 0}$ (b) states.

from the O($4d\ ^3D^0$) state appears not only on the top of the R(c) $4d$ but also at several other Rydberg states with a comparable intensity. Second, we tend to disagree with the assignments of the R(c) nd states used in Ref. [10] which should be reduced by one unit in accordance with the original analysis [17]. Thus the decay of the R(c)nd states to the O($ns\ ^3S$)+O($2p\ ^1D$) limit [see Fig. 5(a)] occurs, in fact, with a change of the principal quantum number.

Several other emission lines have been detected at $h\nu_{exc}=22.3$ eV (556 Å). In addition to the strong fluorescence from the O($3p\ ^5P$) state [Fig. 4(a)] we detect emission lines at 645, 615.6, and 532.9 nm corresponding to the decay from the $5s\ ^5S^0$,$4d\ ^5D^0$, and $5d\ ^5D^0$ states to the $3p\ ^5P$ level, respectively, showing on the complex dissociation processes following the excitation to this resonance. We note that the cascade from these quintet states can partially account for the increase of the intensity of the emission from the $3p\ ^5P$ state, which in turn is reflected in the $3p\ ^5P$ curve of Fig. 4(a).

VI. CONCLUSIONS

We have studied fluorescence in the 400–950 nm region from neutral oxygen atoms formed in neutral photodissociation of O_2 in the excitation range $h\nu_{exc}=15$–25 eV. For $h\nu_{exc}=15$–20.5 eV the strongest emission occurs from the O I $3p\ ^5P$ and $3p\ ^3P$ levels and their excitations functions show a line structure which may be attributed to the O_2 Rydberg series R(A), R(b), and R(B). These experimental results and the follow up calculations suggest that the neutral photodissociation in the 15–20.5 eV range follows from spin-allowed predissociations of the R(A), R(b), and R(B) series mediated by the valence states of triplet symmetry shown in Table I. For $h\nu_{exc}=20.5$–25 eV, emission also occurs from O I (nl) Rydberg states ($n\geqslant 4$) as well as emission from $3p\ ^{3,5}P$, and the structures in the excitation functions partially coincide with that of the O_2 R(c) Rydberg series. However, in view of the high density of states in this energy region, we abandon attempts to try to identify associated predissociating states. It is of interest to compare the present results on O_2 to similar studies of neutral dissociation of N_2 in the 20–30 eV region [18]. In the latter case N_2 Rydberg series were found to be predissociated by a number of non-Rydberg doubly excited states yielding excited N I ($3s\ ^{2,4}P$) and N I ($3p\ ^{2,4}S^0,P^0,D^0$) atoms.

ACKNOWLEDGMENTS

Financial support from The Swedish Natural Science Research Council (NFR) is gratefully acknowledged.

---

[1] W.L. Borst and E.C. Zipf, Phys. Rev. A **4**, 153 (1971).
[2] M.B. Schulman, F.A. Sharpton, Sunggi Chung, Chun C. Lin and L.W. Anderson, Phys. Rev. A **32**, 2100 (1985).
[3] N.J. Mason and W.R. Newell, J. Phys. B **23**, 4641 (1990).
[4] B.R. Lewis, P.M. Dooley, J.P. England, K. Waring, S.T. Gibson, K.G.H. Baldwin, and H. Partridge, Phys. Rev. A **54**, 3923 (1996).
[5] L.C. Lee, R.W. Carlson, D.L. Judge, and M. Ogawa, J. Chem. Phys. **61**, 3261 (1974).
[6] P. Erman, A. Karawajczyk, E. Rachlew-Källne, S. Sorensen, and C. Strömholm, Phys. Scr. **49**, 308 (1994)
[7] A.A. Cafolla, T. Reddish, and J. Comer, J. Phys. B **22**, L273 (1989).
[8] P.M Guyon, A.V. Golovin, C.J.K. Quayle, M. Vervloet, and M. Richard-Viard, Phys. Rev. Lett. **76**, 600 (1996).
[9] M. Ukai, N. Kouchi, K. Kameta, N. Terazawa, Y. Chikahiro, Y. Hatano, and K. Tanaka, Chem. Phys. Lett. **195**, 298 (1992).
[10] M. Ukai, S. Machida, K. Kameta, M. Kitajima, N. Kouchi, Y. Hatano, and K. Ito, Phys. Rev. Lett. **74**, 239 (1995).
[11] P. Erman, A. Karawajczyk, U. Köble, E. Rachlew-Källne, K. Yoshiki Franzen, and L. Veseth, Phys. Rev. Lett. **76**, 4136 (1996).

[12] P. Erman, A. Karawajczyk, E. Rachlew-Källne, M. Stankiewicz, K. Yoshiki Franzen, P. Sannes, and L. Veseth, Phys. Rev. A **55**, 4221 (1997).
[13] P. Sannes and L. Veseth, Phys. Rev. A **56**, 2893 (1997).
[14] L.D. Landau and E.M. Lifshitz, *Quantum Mechanics*, 3rd ed. (Pergamon Press, Oxford, 1962).
[15] E. Nishitani, I. Tanaka, K. Tanaka, T. Kato, and I. Koyano, J. Chem. Phys. **81**, 3429 (1984).
[16] R.J. Buenker and S.D. Peyerimhoff, Chem. Phys. Lett. **34**, 225 (1975).
[17] K. Codling and R.P. Madden, J. Chem. Phys. **42**, 3295 (1965).
[18] P. Erman, A. Karawajczyk, E. Rachlew-Källne, J.Rius i Riu, M. Stankiewicz, and L. Veseth, Phys. Rev. A **60**, 426 (1999).